

# Tuning Electronic Structure to Control Manganese Nitride Activation.

Ryan M. Clarke, and Tim Storr\*

Department of Chemistry, Simon Fraser University, 8888 University Drive, Burnaby, B.C., Canada.

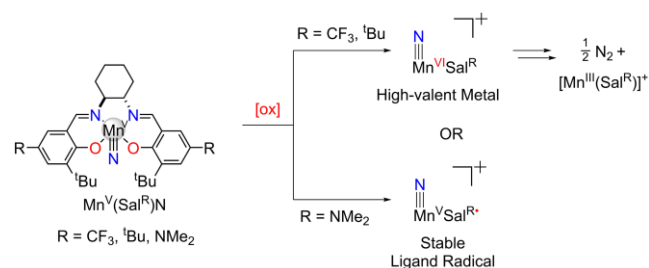
## Supporting Information Placeholder

**ABSTRACT:** Investigation of a series of oxidized nitrido-manganese (V) salen complexes with different para-ring substituents (R = CF<sub>3</sub>, tBu and NMe<sub>2</sub>) demonstrates that nitride activation is dictated by remote ligand electronics. For R = CF<sub>3</sub> and tBu, oxidation affords a Mn(VI) species and nitride activation, with dinitrogen homocoupling accelerated by the more electron withdrawing CF<sub>3</sub> substituent. Employing an electron-donating substituent (R = NMe<sub>2</sub>) results in a localized ligand radical species that is resistant to N-coupling of the nitrides, and is stable in solution at both 195 and 298 K.

Transition metal complexes bearing terminal nitride (N<sup>3-</sup>) ligands are of significant interest due to the key role they may play in the nitrogen fixation process,<sup>1</sup> their importance in stoichiometric nitrene transfer reactions,<sup>2</sup> and their utility as catalysts.<sup>3</sup> In the context of industrial (and biological) nitrogen fixation,<sup>4</sup> there have been a number of important reports of Fe nitride complexes in oxidation states IV,<sup>5</sup> V,<sup>6</sup> and VI,<sup>7</sup> and their reactivities are well documented.<sup>8</sup> In many cases the reactivity of terminal nitride complexes can be rationalized by the nucleophilicity (or electrophilicity) of the nitride ligand, which is determined by both metal and oxidation state, as well as ancillary ligands.<sup>9</sup> Group 8 nitrides of Ru(VI) and Os(VI) react with a variety of nucleophiles<sup>10</sup> due to population of M≡N π\*-antibonding orbitals in the transition state. In addition, reactive electrophilic group 9 terminal nitride complexes of Co,<sup>11</sup> Rh,<sup>12</sup> and Ir<sup>13</sup> have been reported, and a transient terminal nitride of Ni has recently been described.<sup>14</sup> In contrast to the reactivity of late metal nitrides, early metal nitrides are generally more stable, and are often a product of N<sub>2</sub> activation reactions.<sup>15</sup> In some cases, early transition metal nitrides react as nucleophiles.<sup>16</sup> Terminal nitrides of Mn(V) exhibit intermediate reactivity between their early and late transition metal analogues, and have found utility as nitrene transfer reagents.<sup>2b</sup> Early work by Groves demonstrated nitrene transfer from a nitridomanganese(V) porphyrin complex to cyclooctene upon activation with trifluoroacetic anhydride (TFAA).<sup>17</sup> This reactivity was extended to nitridomanganese(V) salen complexes as a means of nitrene transfer to other electron rich alkenes, as well as silyl enol ethers.<sup>18</sup> Despite their synthetic utility, all examples require the addition of Lewis acids such as TFAA or tosic anhydride; likely to activate the nitride by conversion to

the corresponding imide before group transfer to the substrate.<sup>19</sup> Nitridomanganese(V) salen complexes have also been employed as a reagent in the synthesis of other metal-nitrido fragments.<sup>20</sup> Herein, we investigate the oxidative activation of a series of Mn(V) nitrides in which the resulting reactivity is tuned by the electronic properties of the ancillary ligand (Scheme 1). We employ the tetradentate salen due to its facile and highly modular synthesis, allowing for changes in the electron-donating ability of the ligand without altering the geometry at the metal center. More importantly, metal complexes of salen-type ligands have the potential for redox activity at either the ligand or the metal center upon one-electron oxidation,<sup>21</sup> permitting investigation of the resultant reactivity upon oxidation of either metal or ligand in a series of nitridomanganese (V) complexes.

**Scheme 1. Oxidation of Mn<sup>V</sup> nitride complexes to afford high valent metal or ligand radical electronic structures. Subsequent homocoupling affords N<sub>2</sub> in the case of the Mn<sup>VI</sup> complexes.**



Of the three nitridomanganese(V) salen complexes studied herein, Mn(Sal<sup>tBu</sup>)N, and Mn(Sal<sup>CF<sub>3</sub></sup>)N were prepared from the corresponding Mn chloride complexes using NH<sub>4</sub>OH as described by Carreira and co-workers.<sup>18d</sup> While Mn(Sal<sup>NMe<sub>2</sub></sup>)N could also be prepared in this manner, photolysis of the precursor azido complex afforded Mn(Sal<sup>NMe<sub>2</sub></sup>)N in higher yield. All three complexes are isolated as microcrystalline solids with diamagnetic d<sup>2</sup> ground states as expected for Mn(V) nitrides in tetragonal ligand fields.<sup>22</sup> The solid-state structures of the two new nitridomanganese(V) complexes Mn(Sal<sup>CF<sub>3</sub></sup>)N and Mn(Sal<sup>NMe<sub>2</sub></sup>)N are depicted in Figs. S1 and S2, while the solid-state structure of Mn(Sal<sup>tBu</sup>)N was previously reported by Jorgensen.<sup>23</sup> Cyclic voltammetry (CV) experiments on the three complexes

revealed an oxidation process that was tunable by *ca.* 480 mV, and which correlates well with the respective Hammett parameters of the *para*-substituents (Fig. S3).<sup>21b, 24</sup> Analysis of the scan-rate dependence suggested an EC process for both tBu and CF<sub>3</sub> derivatives, while the NMe<sub>2</sub> redox couple remained quasi-reversible at all scan rates investigated (Figs. S4 and S5). The relatively low oxidation potential of the three complexes allowed for their one electron oxidation with AgSbF<sub>6</sub>.<sup>25</sup> Oxidation of a green solution of Mn(Sal<sup>tBu</sup>)N at 298 K resulted in an immediate color change to orange-brown, and characterization of the recrystallized product showed quantitative formation of the high-spin Mn(III) complex [Mn(Sal<sup>tBu</sup>)]<sup>+</sup>[SbF<sub>6</sub><sup>-</sup>] (Figs. S7 and S8). This result suggested that oxidation of Mn(Sal<sup>tBu</sup>)N resulted in rapid loss of the nitride ligand to afford the crystallographically characterized [Mn(Sal<sup>tBu</sup>)]<sup>+</sup>[SbF<sub>6</sub><sup>-</sup>] product. Lau has studied the N-N homocoupling reactivity extensively of various complexes of Ru(VI), Os(VI) and Mn(V) with Schiff-base ligands.<sup>26</sup> While both Ru(VI) and Os(VI) complexes undergo N-N coupling reactions in the presence of N-heterocyclic ligands,<sup>10h, 27</sup> Mn nitrides have not been observed to couple N<sub>2</sub> directly.<sup>28</sup> Additional examples of dinitrogen coupling reactions from transition metal nitrides include Fe(IV/V) complexes,<sup>5b, 29</sup> an open shell Ir complex and its analogous Rh complex,<sup>12-13</sup> as well as between Os and Mo complexes.<sup>30</sup>

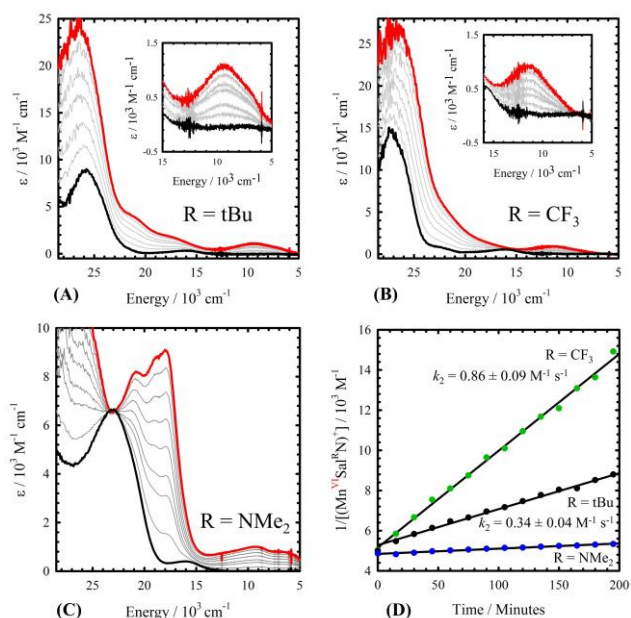


**Figure 1.** (A-C): Oxidation titration data for Mn(Sal<sup>R</sup>)N (black) to the corresponding one-electron oxidized species (red). Intermediate grey lines are measured during the oxidation titrations with [N(C<sub>6</sub>H<sub>3</sub>Br<sub>2</sub>)<sub>3</sub>]<sup>+</sup>[SbF<sub>6</sub><sup>-</sup>]. Insets: enhanced view of the low energy bands for R=tBu and CF<sub>3</sub>. (D): Representative kinetic decay data for the three complexes (R = tBu and CF<sub>3</sub>: 195 K, R = NMe<sub>2</sub>: 298 K). Conditions: CH<sub>2</sub>Cl<sub>2</sub>, 0.2 mM complex.

We next endeavored to characterize the oxidized species at low temperature in order to further understand the observed reactivity. Mn(Sal<sup>tBu</sup>)N can be cleanly oxidized at 195 K using the aminium radical chemical oxidant, [N(C<sub>6</sub>H<sub>3</sub>Br<sub>2</sub>)<sub>3</sub>]<sup>+</sup>[SbF<sub>6</sub><sup>-</sup>],<sup>25</sup> to afford a species with an electronic structure that differs from either the starting material or decay product (Fig. 1A). Upon oxidation, formation of a low-intensity band is ob-

served at 9300 cm<sup>-1</sup> ( $\epsilon = 1100 \text{ M}^{-1} \text{ cm}^{-1}$ ). Time-Dependent DFT analysis predicts the low energy band to have ligand-to-metal charge transfer (LMCT) character (Fig S9).

A sample of the oxidized species [Mn(Sal<sup>tBu</sup>)N]<sup>+</sup> was then analyzed by EPR spectroscopy at 100 K. The EPR spectrum of [Mn(Sal<sup>tBu</sup>)N]<sup>+</sup> shows that the oxidation is metal-based, affording a Mn(VI) species (Fig. 2). The spectrum displays a typical axial splitting pattern for a *d*<sup>1</sup> metal ion (*d*<sub>xy</sub><sup>1</sup> ground state) with hyperfine coupling to a single <sup>55</sup>Mn (*I* = 5/2) nucleus (*A*<sub>zz</sub> = 533 MHz, *A*<sub>xx</sub> = *A*<sub>yy</sub> = 182 MHz). These values are in close agreement with two Mn(VI) complexes previously reported by Wieghardt and co-workers.<sup>31</sup>

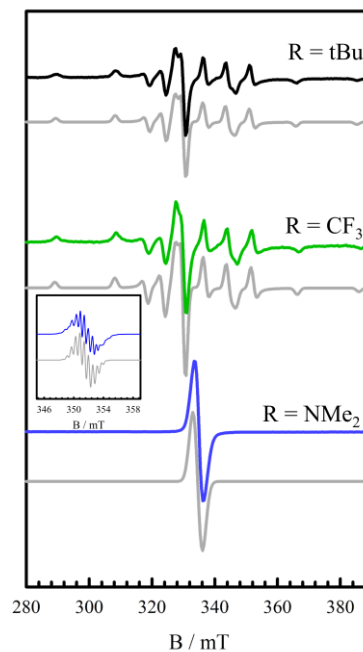


**Figure 2.** X-band EPR spectra of [Mn(Sal<sup>R</sup>)N]<sup>+</sup> recorded in frozen CH<sub>2</sub>Cl<sub>2</sub> at 0.4 mM. Top: R = tBu; Middle: R = CF<sub>3</sub>; Bottom: R = NMe<sub>2</sub>. Grey lines represent simulations to the experimental data. Inset: Room temperature spectrum of R = NMe<sub>2</sub>. Conditions: frequency = 9.38 GHz; power = 2.0 mW; modulation frequency = 100 kHz; modulation amplitude = 0.6 mT; T = 100 K.

**Table 1.** EPR simulation parameters for the three oxidized complexes. Hyperfine values (A) are in MHz.

	<i>g</i> <sub>zz</sub>	<i>g</i> <sub>xx</sub> = <i>g</i> <sub>yy</sub>	<i>A</i> <sub>zz</sub>	<i>A</i> <sub>xx</sub> = <i>A</i> <sub>yy</sub>
R = tBu	1.985	1.995	533	181
R = CF <sub>3</sub>	1.984	1.995	540	187
R = NMe <sub>2</sub> (100 K)	2.003			
R = NMe <sub>2</sub> (298 K)	2.003	<i>A</i> <sub>N1</sub> = 13.5; 6 × <i>A</i> <sub>H1</sub> = 16.7; <i>A</i> <sub>H2</sub> = 2.8; <i>A</i> <sub>H3</sub> = 0.8; <i>A</i> <sub>Mn</sub> = 4.2		

Despite being able to characterize the reactive Mn(VI) intermediate, we observed slow decay (*t*<sub>1/2</sub> = 4 hours at 0.2 mM) of this species at 195 K. The decay was fit to a second order process (Fig. S10, *k*<sub>2</sub> = 0.34 ± 0.04 M<sup>-1</sup> s<sup>-1</sup>), in line with a reac-

tion mechanism that involves two molecules of  $[\text{Mn}(\text{Sal}^{\text{tBu}})\text{N}]^+$  coupling to produce  $\text{N}_2$  and two molecules of  $[\text{Mn}(\text{Sal}^{\text{tBu}})][\text{SbF}_6]$ . In order to confirm that the mechanism for nitride loss was a result of an intermolecular reaction between two molecules of  $[\text{Mn}(\text{Sal}^{\text{tBu}})\text{N}]^+$ , we prepared the 50%  $^{15}\text{N}$  labelled complex. We performed GC-MS measurements in order to monitor the gas evolved after oxidation of  $\text{Mn}(\text{Sal}^{\text{tBu}})\text{N}$ . Although difficult to eliminate atmospheric  $^{14}\text{N}^{14}\text{N}$  from the instrument, we detected  $^{14}\text{N}^{15}\text{N}$  and  $^{15}\text{N}^{15}\text{N}$  in a 2:1 ratio, as expected for an intermolecular reaction mechanism involving two molecules of 50%  $^{15}\text{N}$  labelled  $\text{Mn}(\text{Sal}^{\text{tBu}})\text{N}$  (Table S3, Fig. S11).

We next investigated activation of the two additional Mn(V) nitride complexes with salen *para* substituents of contrasting electron donating abilities ( $\text{CF}_3$  and  $\text{NMe}_2$ ). Oxidation of  $\text{Mn}(\text{Sal}^{\text{CF}_3})\text{N}$  at 195 K resulted in the appearance of similar spectral features to the tBu derivative, with the low energy band at slightly higher energy ( $11600\text{ cm}^{-1}$ ). As expected, EPR analysis confirmed that oxidation of the  $\text{CF}_3$  derivative resulted in metal-based oxidation to Mn(VI), with nearly identical simulation parameters as the tBu derivative (Table 1).  $[\text{Mn}(\text{Sal}^{\text{CF}_3})\text{N}]^+$  also decays at low temperature, following a second order decay model (Fig. 1D, Fig. S12). The rate constant ( $k_2 = 0.86 \pm 0.09\text{ M}^{-1}\text{ s}^{-1}$ ) is approximately 2.5 times larger in comparison to the tBu derivative, which can be attributed to the change in auxiliary ligand electronics (*vide infra*).  $^{15}\text{N}$  isotopic labelling of the nitride again suggests an intermolecular reaction mechanism for the  $\text{CF}_3$  derivative (Table S4, Fig. S13).

We next installed an electron donating  $\text{NMe}_2$  group at the *para* position of the salen ligand. Examination of the CV spectrum of  $\text{Mn}(\text{Sal}^{\text{NMe}_2})\text{N}$  does not suggest an EC process based on evaluation of the scan-rate dependence (Fig. S4). Low temperature oxidation results in unique vis-NIR spectral features in comparison to the tBu and  $\text{CF}_3$  derivatives. Two broad, low-energy transitions at  $6500\text{ cm}^{-1}$  ( $800\text{ M}^{-1}\text{ cm}^{-1}$ ) and  $9500\text{ cm}^{-1}$  ( $1000\text{ M}^{-1}\text{ cm}^{-1}$ ) are present in the spectrum, as well as an envelope of transitions between  $15,000\text{--}22,000\text{ cm}^{-1}$  (Fig. 1C). TD-DFT reveals these transitions to be largely ligand based, and their absence in the spectra of the previous derivatives suggests a change in electronic structure. Indeed, collection of the EPR spectrum in frozen  $\text{CH}_2\text{Cl}_2$  reveals that the locus of oxidation for  $[\text{Mn}(\text{Sal}^{\text{NMe}_2})\text{N}]^+$  is ligand-based, exhibiting an isotropic ligand radical signal centered at  $g = 2.003$  (Fig. 2). This demonstrates that sufficiently electron-donating *para* substituents are capable of re-ordering the relative energies of redox-active orbitals such that oxidation is no-longer metal-centered, but ligand-centered in this derivative. In addition, unlike the tBu and  $\text{CF}_3$  derivatives, the oxidized  $\text{NMe}_2$  derivative is resistant to homocoupling as the oxidized complex is stable at 195 K; and only decays minimally over a 48-hour period at 298 K (Fig. 1D, Fig. S14). The  $\text{Mn}=\text{N}$  stretching band at  $1045\text{ cm}^{-1}$  persists after oxidation with  $\text{AgSbF}_6$  at room temperature. Furthermore, the decay at 298 K is not well modelled by second order kinetics, suggesting the instability of the oxidized complex is due to a mechanism other than N-coupling.<sup>32</sup> Unfortunately, we have been unable to isolate x-ray quality crystals of the oxidized complex. In a recent report, van der Vlugt and co-workers describe the participation of a redox-active ligand in the formation of a Ru trimer with bridging nitrido ligands,<sup>33</sup> high-

lighting the alternative reactivity pathways that redox-active ligands may impose on transition metal nitrido complexes. We aimed to investigate the degree of radical localization for  $[\text{Mn}(\text{Sal}^{\text{NMe}_2})\text{N}]^+$  via EPR analysis at 298 K (Fig. 2 - inset). The EPR spectrum is simulated by considering significant hyperfine interactions to one  $\text{NMe}_2$  group, with smaller hyperfine couplings to Mn and two phenoxy protons (Table 1). Thus, the EPR pattern at 298 K provides experimental verification of a localized ligand radical electronic structure for  $[\text{Mn}(\text{Sal}^{\text{NMe}_2})\text{N}]^+$ .

Theoretical calculations on the oxidized species match with experimental findings, predicting a Mn(VI) ( $d_{xy}$ ) ground state for  $\text{R} = \text{CF}_3$  and tBu, and formation of a localized ligand radical for  $\text{R} = \text{NMe}_2$  (Fig. 3 and S17). Natural bond order (NBO) analysis is consistent with a covalent  $\text{Mn}=\text{N}$  triple bond in the oxidized forms (Tables S7 and S8), with the Mayer bond orders decreasing slightly in the order  $\text{NMe}_2 > \text{tBu} > \text{CF}_3$  (2.868, 2.732, 2.730). The negative spin density localized to the nitride in  $\text{R} = \text{tBu}$  (-0.20) and  $\text{R} = \text{CF}_3$  (-0.24) can be rationalized by considering the  $\text{Mn}-\text{N}$  bond as a combination of  $\text{Mn}(\text{VI})\equiv\text{N}^{3-}$  ( $S_{\text{Mn}} = 1/2$ )  $\leftrightarrow$   $\text{Mn}(\text{V})=\text{N}\cdot$  ( $S_{\text{N}} = 1/2$ ) resonance forms (Fig. 3).<sup>6a, 29, 34</sup> A nitridyl radical resonance form, which could be slightly favored for  $\text{R} = \text{CF}_3$ , provides further support for a radical coupling pathway to produce  $\text{N}_2$  in this study.

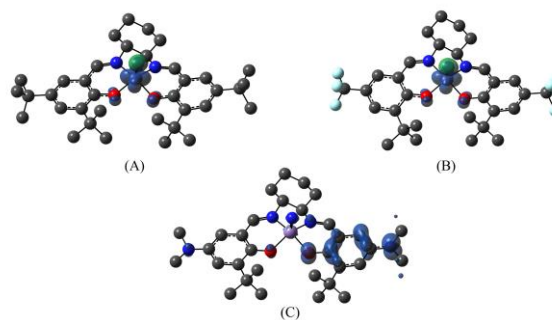


**Figure 3.** Spin density plots for the 3 oxidized complexes. (A)  $[\text{Mn}(\text{Sal}^{\text{tBu}})\text{N}]^+$ ; (B)  $[\text{Mn}(\text{Sal}^{\text{CF}_3})\text{N}]^+$ ; (C)  $[\text{Mn}(\text{Sal}^{\text{NMe}_2})\text{N}]^+$ . See experimental section for details.

This study provides key insight into the role of ligand electronics in the nitride activation process, with the nitride precursors readily synthesized from oxidative conditions in the presence of  $\text{NH}_4\text{OH}$ . Further efforts are needed to model the reaction pathway and assess the possibility of accessing and activating  $\text{NH}_3$  adducts of electron-deficient Mn salen systems for  $\text{H}_2$  generation, as well as the potential for these systems to activate C-H bonds through radical reaction pathways.

## ASSOCIATED CONTENT

### Supporting Information

Full experimental details, x-ray structures, CV and DPV data, full triplicate kinetics analysis, DFT assignment of the UV-Vis-NIR low energy bands, GC-MS headspace analysis, NBO analysis as well as optimized DFT coordinates for neutral and oxidized complexes. The supporting information is available free of charge on the ACS Publications website.

## AUTHOR INFORMATION



## Corresponding Author

\*[tim\\_storr@sfu.ca](mailto:tim_storr@sfu.ca)

## Notes

The authors declare no competing financial interests.

## ACKNOWLEDGMENTS

This work is supported by a National Sciences and Engineering Research Council (NSERC) Discovery Grant (T.S.). R.M.C. thanks NSERC for a postgraduate fellowship. Compute Canada and Westgrid are thanked for access to computational resources. The authors gratefully acknowledge the assistance of Kathleen Prosser and Charles Walsby at SFU, and Fabrice Thomas at Université Grenoble-Alpes for EPR acquisition; John Thompson and Jeffery Ovens for X-ray structure solution assistance; and Paul Mulyk for assistance with GC-MS measurements.

## REFERENCES

- (1) (a) Yandulov, D. V.; Schrock, R. R., *Science* **2003**, *301*, 76; (b) Arashiba, K.; Kinoshita, E.; Kuriyama, S.; Eizawa, A.; Nakajima, K.; Tanaka, H.; Yoshizawa, K.; Nishibayashi, Y., *J. Am. Chem. Soc.* **2015**, *137*, 5666.
- (2) (a) Curley, J. J.; Sceats, E. L.; Cummins, C. C., *J. Am. Chem. Soc.* **2006**, *128*, 14036; (b) Du Bois, J.; Tomooka, C. S.; Hong, J.; Carreira, E. M., *Acc. Chem. Res.* **1997**, *30*, 364.
- (3) (a) Gdula, R. L.; Johnson, M. J. A., *J. Am. Chem. Soc.* **2006**, *128*, 9614; (b) Chisholm, M. H.; Delbridge, E. E.; Kidwell, A. R.; Quinlan, K. B., *Chem. Commun.* **2003**, 126.
- (4) Ertl, G., *Catalytic Ammonia Synthesis*. Plenum: New York, 1991.
- (5) (a) Vogel, C.; Heinemann, F. W.; Sutter, J.; Anthon, C.; Meyer, K., *Angew. Chem.* **2008**, *120*, 2721; (b) Betley, T. A.; Peters, J. C., *J. Am. Chem. Soc.* **2004**, *126*, 6252; (c) Rohde, J.-U.; Betley, T. A.; Jackson, T. A.; Saouma, C. T.; Peters, J. C.; Que, L., *Inorg. Chem.* **2007**, *46*, 5720; (d) Scepaniak, J. J.; Young, J. A.; Bontchev, R. P.; Smith, J. M., *Angew. Chem. Int. Ed.* **2009**, *48*, 3158; (e) Scepaniak, J. J.; Fulton, M. D.; Bontchev, R. P.; Duesler, E. N.; Kirk, M. L.; Smith, J. M., *J. Am. Chem. Soc.* **2008**, *130*, 10515.
- (6) (a) Aliaga-Alcalde, N.; DeBeer George, S.; Mienert, B.; Bill, E.; Wieghardt, K.; Neese, F., *Angew. Chem. Int. Ed.* **2005**, *44*, 2908; (b) Meyer, K.; Bill, E.; Mienert, B.; Weyhermüller, T.; Wieghardt, K., *J. Am. Chem. Soc.* **1999**, *121*, 4859; (c) Scepaniak, J. J.; Vogel, C. S.; Khusniyarov, M. M.; Heinemann, F. W.; Meyer, K.; Smith, J. M., *Science* **2011**, *331*, 1049.
- (7) Berry, J. F.; Bill, E.; Bothe, E.; George, S. D.; Mienert, B.; Neese, F.; Wieghardt, K., *Science* **2006**, *312*, 1937.
- (8) (a) Lee, W.-T.; Juarez, R. A.; Scepaniak, J. J.; Muñoz, S. B.; Dickie, D. A.; Wang, H.; Smith, J. M., *Inorg. Chem.* **2014**, *53*, 8425; (b) Scepaniak, J. J.; Bontchev, R. P.; Johnson, D. L.; Smith, J. M., *Angew. Chem. Int. Ed.* **2011**, *50*, 6630; (c) Muñoz, S. B.; Lee, W.-T.; Dickie, D. A.; Scepaniak, J. J.; Subedi, D.; Pink, M.; Johnson, M. D.; Smith, J. M., *Angew. Chem. Int. Ed.* **2015**, *54*, 10600.
- (9) Smith, J. M., *Reactive Transition Metal Nitride Complexes*. In *Progress in Inorganic Chemistry Volume 58*, John Wiley & Sons, Inc.: 2014; pp 417.
- (10) (a) Maestri, A. G.; Cherry, K. S.; Tboni, J. J.; Brown, S. N., *J. Am. Chem. Soc.* **2001**, *123*, 7459; (b) Brown, S. N., *J. Am. Chem. Soc.* **1999**, *121*, 9752; (c) Crevier, T. J.; Lovell, S.; Mayer, J. M.; Rheingold, A. L.; Guzei, I. A., *J. Am. Chem. Soc.* **1998**, *120*, 6607; (d) Crevier, T. J.; Mayer, J. M., *J. Am. Chem. Soc.* **1998**, *120*, 5595; (e) Meyer, T. J.; Huynh, M. H. V., *Inorg. Chem.* **2003**, *42*, 8140; (f) Xie, J.; Man, W.-L.; Wong, C.-Y.; Chang, X.; Che, C.-M.; Lau, T.-C., *J. Am. Chem. Soc.* **2016**, *138*, 5817; (g) Man, W.-L.; Lam, W. W. Y.; Kwong, H.-K.; Yiu, S.-M.; Lau, T.-C., *Angew. Chem. Int. Ed.* **2012**, *51*, 9101; (h) Man, W.-L.; Tang, T.-M.; Wong, T.-W.; Lau, T.-C.; Peng, S.-M.; Wong, W.-T., *J. Am. Chem. Soc.* **2004**, *126*, 478; (i) Man, W.-L.; Lam, W. W. Y.; Yiu, S.-M.; Lau, T.-C.; Peng, S.-M., *J. Am. Chem. Soc.* **2004**, *126*, 15336.
- (11) Zolnhofer, E. M.; Käb, M.; Khusniyarov, M. M.; Heinemann, F. W.; Maron, L.; van Gestel, M.; Bill, E.; Meyer, K., *J. Am. Chem. Soc.* **2014**, *136*, 15072.
- (12) Scheibel, M. G.; Wu, Y.; Stückl, A. C.; Krause, L.; Carl, E.; Stalke, D.; de Bruin, B.; Schneider, S., *J. Am. Chem. Soc.* **2013**, *135*, 17719.
- (13) (a) Scheibel, M. G.; Askevold, B.; Heinemann, F. W.; Reijerse, E. J.; de Bruin, B.; Schneider, S., *Nat Chem* **2012**, *4*, 552; (b) Schöffel, J.; Rogachev, A. Y.; DeBeer George, S.; Burger, P., *Angew. Chem. Int. Ed.* **2009**, *48*, 4734.
- (14) Vreeken, V.; Siegler, M. A.; de Bruin, B.; Reek, J. N. H.; Lutz, M.; van der Vlugt, J. I., *Angew. Chem. Int. Ed.* **2015**, *54*, 7055.
- (15) (a) Laplaza, C. E.; Cummins, C. C., *Science* **1995**, *268*, 861; (b) Laplaza, C. E.; Johnson, M. J. A.; Peters, J. C.; Odom, A. L.; Kim, E.; Cummins, C. C.; George, G. N.; Pickering, I. J., *J. Am. Chem. Soc.* **1996**, *118*, 8623; (c) Curley, J. J.; Cook, T. R.; Reece, S. Y.; Müller, P.; Cummins, C. C., *J. Am. Chem. Soc.* **2008**, *130*, 9394.
- (16) (a) Thompson, R.; Tran, B. L.; Ghosh, S.; Chen, C.-H.; Pink, M.; Gao, X.; Carroll, P. J.; Baik, M.-H.; Mindiola, D. J., *Inorg. Chem.* **2015**, *54*, 3068; (b) Eikey, R. A.; Abu-Omar, M. M., *Coord. Chem. Rev.* **2003**, *243*, 83.
- (17) Groves, J. T.; Takahashi, T., *J. Am. Chem. Soc.* **1983**, *105*, 2073.
- (18) (a) Ho, C.-M.; Lau, T.-C.; Kwong, H.-L.; Wong, W.-T., *J. Chem. Soc. Dalton Trans.* **1999**, 2411; (b) Minakata, S.; Ando, T.; Nishimura, M.; Ryu, I.; Komatsu, M., *Angew. Chem. Int. Ed.* **1998**, *37*, 3392; (c) Du Bois, J.; Tomooka, C. S.; Hong, J.; Carreira, E. M., *J. Am. Chem. Soc.* **1997**, *119*, 3179; (d) Du Bois, J.; Hong, J.; Carreira, E. M.; Day, M. W., *J. Am. Chem. Soc.* **1996**, *118*, 915.
- (19) Bottomley, L. A.; Neely, F. L., *J. Am. Chem. Soc.* **1988**, *110*, 6748.
- (20) (a) Golubkov, G.; Gross, Z., *J. Am. Chem. Soc.* **2005**, *127*, 3258; (b) Hedegaard, E. D.; Schau-Magnussen, M.; Bendix, J., *Inorg. Chem. Commun.* **2011**, *14*, 719; (c) Bendix, J.; Wilson, S. R.; Prussak-Wieckowska, T., *Acta Crystallogr. Sect. C-Cryst. Struct. Commun.* **1998**, *54*, 923; (d) Bendix, J., *J. Am. Chem. Soc.* **2003**, *125*, 13348; (e) Birk, T.; Bendix, J., *Inorg. Chem.* **2003**, *42*, 7608; (f) Bendix, J.; Birk, T.; Weyhermüller, T., *Dalton Trans.* **2005**, 2737.
- (21) (a) Storr, T.; Wasinger, E. C.; Pratt, R. C.; Stack, T. D. P., *Angew. Chem. Int. Ed.* **2007**, *46*, 5198; (b) Chiang, L.; Herasymchuk, K.; Thomas, F.; Storr, T., *Inorg. Chem.* **2015**, *54*, 5970; (c) Kurahashi, T.; Fujii, H., *J. Am. Chem. Soc.* **2011**, *133*, 8307; (d) Orio, M.; Jarjayes, O.; Kanso, H.; Philouze, C.; Neese, F.; Thomas, F., *Angew. Chem. Int. Ed.* **2010**, *49*, 4989.
- (22) (a) Chang, C. J.; Connick, W. B.; Low, D. W.; Day, M. W.; Gray, H. B., *Inorg. Chem.* **1998**, *37*, 3107; (b) Kropp, H.; King, A. E.; Khusniyarov, M. M.; Heinemann, F. W.; Lancaster, K. M.; DeBeer, S.; Bill, E.; Meyer, K., *J. Am. Chem. Soc.* **2012**, *134*, 15538.
- (23) Svenstrup, N.; Bogeveg, A.; G. Hazell, R.; Anker Jorgensen, K., *J. Chem. Soc., Perkin Trans.* **1999**, 1559.
- (24) (a) Hansch, C.; Leo, A.; Taft, R. W., *Chem. Rev.* **1991**, *91*, 165; (b) Hewage, J. S.; Wanniarachchi, S.; Morin, T. J.; Liddle, B. J.; Banaszynski, M.; Lindeman, S. V.; Bennett, B.; Gardinier, J. R., *Inorg. Chem.* **2014**, *53*, 10070; (c) Solis, B. H.; Hammes-Schiffer, S., *J. Am. Chem. Soc.* **2011**, *133*, 19036.
- (25) Connelly, N. G.; Geiger, W. E., *Chem. Rev.* **1996**, *96*, 877.
- (26) Man, W.-L.; Lam, W. W. Y.; Lau, T.-C., *Acc. Chem. Res.* **2014**, *47*, 427.
- (27) (a) Man, W.-L.; Chen, G.; Yiu, S.-M.; Shek, L.; Wong, W.-Y.; Wong, W.-T.; Lau, T.-C., *Dalton Trans.* **2010**, *39*, 11163; (b) Man, W.-L.; Kwong, H.-K.; Lam, W. W. Y.; Xiang, J.; Wong, T.-W.; Lam, W.-H.; Wong, W.-T.; Peng, S.-M.; Lau, T.-C., *Inorg. Chem.* **2008**, *47*, 5936.
- (28) Yiu, S.-M.; Lam, W. W. Y.; Ho, C.-M.; Lau, T.-C., *J. Am. Chem. Soc.* **2007**, *129*, 803.
- (29) Krahe, O.; Bill, E.; Neese, F., *Angew. Chem. Int. Ed.* **2014**, *53*, 8727.
- (30) Seymore, S. B.; Brown, S. N., *Inorg. Chem.* **2002**, *41*, 462.
- (31) (a) Bendix, J.; Meyer, K.; Weyhermüller, T.; Bill, E.; Metzler-Nolte, N.; Wieghardt, K., *Inorg. Chem.* **1998**, *37*, 1767; (b) Meyer, K.; Bendix, J.; Metzler-Nolte, N.; Weyhermüller, T.; Wieghardt, K., *J. Am. Chem. Soc.* **1998**, *120*, 7260.
- (32) The oxidized 50% <sup>15</sup>N labelled [Mn(Sal<sup>NMe2</sup>)N]<sup>+</sup> shows no evidence of homocoupling up to 24 hours by GC-MS (Table S5 and S6, Fig. S15 and S16).
- (33) Bagh, B.; Broere, D. L. J.; Siegler, M. A.; van der Vlugt, J. I., *Angew. Chem. Int. Ed.* **2016**, *55*, 8381.
- (34) (a) Hoffsail Iii, G. E.; Stein, B. W.; Subedi, D.; Smith, J. M.; Kirk, M. L.; Hoffman, B. M., *J. Am. Chem. Soc.* **2014**, *136*, 12323; (b) Suarez, A. I. O.; Lyaskovskyy, V.; Reek, J. N. H.; van der Vlugt, J. I.; de Bruin, B., *Angew. Chem. Int. Ed.* **2013**, *52*, 12510.

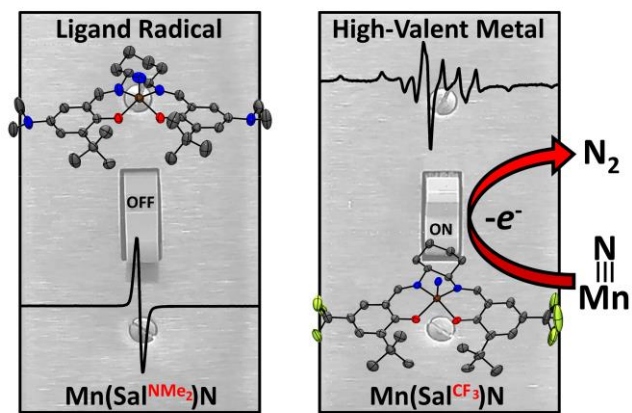


Table of Contents Graphic